

Multi-Objective Optimization for Value-Sensitive and Sustainable Basket Recommendations

Thomas Asikis
asikist@ethz.ch

¹Chair of Computational Social Science, ETH Zurich, Zurich,
Switzerland,

November 12, 2021

Abstract

Sustainable consumption aims to minimize the environmental and societal impact of the use of services and products. Over-consumption of services and products leads to potential natural resource exhaustion and societal inequalities, as access to goods and services becomes more challenging. In everyday life, a person can simply achieve more sustainable purchases by drastically changing their lifestyle choices and potentially going against their personal values or wishes. Conversely, achieving sustainable consumption while accounting for personal values is a more complex task, as potential trade-offs arise when trying to satisfy environmental and personal goals. This article focuses on value-sensitive design of recommender systems, which enable consumers to improve the sustainability of their purchases while respecting their personal values. Value-sensitive recommendations for sustainable consumption are formalized as a multi-objective optimization problem, where each objective represents different sustainability goals and personal values. Novel and existing multi-objective algorithms calculate solutions to this problem. The solutions are proposed as personalized sustainable basket recommendations to consumers. These recommendations are evaluated on a synthetic dataset, which comprises three established real-world datasets from relevant scientific and organizational reports. The synthetic dataset contains quantitative data on product prices, nutritional values and environmental impact metrics, such as greenhouse gas emissions and water footprint. The recommended baskets are highly similar to consumer purchased baskets and aligned with both sustainability goals and personal values relevant to health, expenditure and taste. Even when consumers would accept only a fraction of recommendations, a considerable reduction of environmental impact is observed.

1 Introduction

Sustainable Development Goals [36] (SDG) have been proposed by the United Nations (UN) to describe several sustainability criteria in form of goals, tasks, and scenarios. Environment and society related sustainability goals can be broken down to numerous constraints and objectives [28, 7] that affect everyday decisions, such reduction of CO₂ emission with everyday activities. Making an optimal decision with respect to such constraints and objectives often introduces potential trade-offs, e.g. making a decision that minimizes CO₂ emissions of a certain activity may increase its water footprint. Including personal values, such as preference/taste or budget constraints may introduce even more trade-offs and make the decision process more challenging. Several multi-objective optimization methods that tackle such problems are considered under the umbrella term of Artificial Intelligence (AI) [19, 29, 1] AI is expected to play a key role [38] in solving complex challenges arising from SDGs. Nevertheless, applying AI may also inhibit sustainability challenges relevant to value-sensitive design, namely challenges related to: (i) unequal distribution of resources, (ii) loss individual of autonomy and privacy, and (iii) increased emissions from calculations [38, 20]. Value-sensitive design of AI systems aims to address such challenges.

Consumption is one of the main driving factors of industrial production, and thus has great environmental and societal impact [16]. This impact is the aggregated individual impact of everyday consumer choices. Every day, consumers are urged to take several decisions to fulfill their personal goals and values, mainly originating from individual needs and wishes. Shopping decisions often aim to satisfy several criteria, such as the taste, the ability of purchased products to be combined together, available consumer budget, and health implications of consuming the product. Trade-offs arise when optimizing for personal values, e.g. when a consumer needs to decide between a healthier and cheaper product. Such trade-offs are mainly addressed by multi-objective optimization in modern recommender systems [43]. Value-sensitive design can be applied to create systems that support individual decisions when resolving these trade-offs [3]. Following a value-sensitive design indicates that personal values can be incorporated in the system design, often introducing new constraints and objectives to the optimization. Thus, combining value-sensitive design and sustainable decision-making results in even more complex and challenging trade-off optimization problems.

Self-determined systems that are based on retailer data, crowd-sourcing, and expert input, have already been successfully tested in the past. Although the effect of sustainable recommendations on individual purchases is often observed [30, 2, 5], there is little quantitative analysis on the collective impact of more sustainable decisions on emissions, pollution, resource usage, and personal values. Existing analytical models that often estimate such impact do not deal or represent real-world data on individual/microscopic level, but rather consists mostly of theoretical economical and climate models that evaluate sustainability on a macroscopic or societal level [28, 35]. A welfare objective function

that includes analytical terms representing satisfaction from consumption and environmental pollution is often optimized [31, 35]. The optimization outcomes are then used in analysis and policy making. Although macroscopic and/or centralized models can provide useful insights, it may not be possible to anticipate for errors in estimation of individual objective functions and system state. Criticism on centralized models often focuses on poor practical applications and potential high estimation errors [6], as well as potential challenges to addressing personal values and morals [13]. Data-oriented approaches that focus on individual/microscopic level can be directly applied in real-world scenarios in the form of mobile applications and website recommender systems [3]. Relevant recommender systems and analyses mainly focus on diets or single product recommendations [1, 34].

The main contributions of the current article are to: (i) propose and formalize a new real-world multi-objective optimization problem for recommendations of personalized sustainable baskets, (ii) create and analyze a novel synthetic dataset based on sustainability and consumer real-world data, (iii) propose effective existing baselines for this problem, and (iv) design and implement a novel deep learning framework for mixed integer programming multi-objective optimization problems. In Section 2 an explicit formalization of the proposed optimization problem is presented. Therein constraints, trade-offs, and objectives originating from value-sensitive design and SDGs are combined to form a multi-objective optimization problem. The proposed dataset structure can be used to generate similar real-world datasets by online retailers to enable value-sensitive sustainable recommendations. Section 3.1 introduces a novel deep learning architecture, termed gradient guided genetic algorithm (G3A), which combines the ability of evolutionary strategies to solve complex multi-objective problems and the ability of Neural Ordinary Differential Equation Control (NODEC) [2, 5] to efficiently and timely control complex processes, such as genetic evolution. Section 4 presents the results of experimental evaluation of G3A and other multi-objective optimization algorithms on the problem discussed in Section 2. Section 5 concludes the article.

All relevant data and code for the current article are reported in Sections A and B and will be available online. Appendix Section E summarizes the creation and analysis of the synthetic dataset, which combines consumer transactions and product data from “The Complete Journey Dataset” by the Dunnhumby grocery store [14], emission and resource usage indicators from Ref. [32], and nutrition information from Food Agricultural Organization Food Balance Sheets [24]. Further technical details, such as hyper-parameters, training time, and baseline comparison are found in the Appendix Sections D and E.

2 Personalized Sustainable Baskets

Value-sensitive sustainable recommendations are formalized as a multi-objective optimization problem of selecting combinations of discrete quantities over $N = 132$ distinct products. First, an intended basket is defined as the purchased

weekly basket, i.e. a vector of non-negative integer product quantities $\mathbf{x}_{k,q}^* \in \mathbb{N}_0^N$ for a specific household k at week q . In a real-world application, where the purchased basket is not known, the user may provide an intended basket via a shopping list interface or an e-shop basket interface. For brevity, week q and household k indices are omitted from the basket vector, as the proposed multi-objective optimization calculations do not require values of intended baskets that were purchased in the past or from other households. The intended basket \mathbf{x}^* is considered as the initial solution of the presented problem and is also considered as the basket that represents consumer taste and nutritional goals. For the current study an ordered set C of $|C| = 11$ of possible recommendation features is considered, where a feature index $j = 1$ indicates the corresponding feature as shown in Table 2.

j	Feature	Unit	Scope	Target
1	Cosine similarity	-	Personal	Max.
2	Cost	Dollars (\$)	Personal	Min.
3	Energy	kilo Calories (kCal)	Personal	Pres.
4	Protein	grams(g)	Personal	Pres.
5	Fat	grams(g)	Personal	Pres.
6	GHG emissions	CO ₂ kg eq.	Environment	Min.
7	Acidification pollution	SO ₂ kg eq.	Environment	Min.
8	Eutrophication pollution	PO ₄ ⁻³ kg eq.	Environment	Min.
9	Land use	m ²	Environment	Min.
10	Water usage	L	Environment	Min.
11	Stressed water usage	L	Environment	Min.

TABLE 2: Features relevant to objectives for basket selection. The first column shows the index of each feature, which also coincides with their position in the ordered set C . Feature, Unit, and Scope columns give a brief overview of the objectives and finally the Target column describes whether the goal of the optimization is to minimize, maximize, or preserve the intended basket value.

The synthetic dataset provides coefficients $c_{i,j}$, which in this study are median values over all transactions in the dataset and describe the corresponding feature j quantity $c_{i,j}$ per unit for each product i . Therefore, for a basket \mathbf{x} , one can calculate the total quantity for a specific feature as

$$v_j(\mathbf{x}) = \sum_{i=1}^N c_{i,j} x_i. \quad (1)$$

When designing the objective functions and comparing recommendations among baselines, often the ratio of total feature quantities between two baskets \mathbf{x}, \mathbf{x}'

$$\rho_j(\mathbf{x}, \mathbf{x}') = \frac{v_j(\mathbf{x})}{v_j(\mathbf{x}')} \quad (2)$$

is used. In particular, most calculations related to environmental and personal objectives use the ratio of a recommendation towards the intended basket $\rho_j(\mathbf{x}, \mathbf{x}^*)$ for a specific feature j .

2.1 Individual Objectives

Consumer taste is the first personal value that is considered as an optimization objective, which is minimized when the recommended basket \mathbf{x} is as similar as possible to the intended basket \mathbf{x}^* . High similarity between a recommended basket \mathbf{x} and the target intended \mathbf{x}^* indicates higher likelihood of a purchase under a counterfactual hypothesis, in which the user would consider recommended baskets before purchase. The first objective function to minimize is a function of the cosine similarity

$$J_1(\mathbf{x}, \mathbf{x}^*) = 1 - \frac{\mathbf{x}^\top \mathbf{x}^*}{\|\mathbf{x}\| \|\mathbf{x}^*\|} \quad (3)$$

Relation (3) is minimized by recommending the intended basket.

The next personal value considered in optimization is a function of cost. In general, it is assumed that individuals would prefer to minimize expenses and select cheaper baskets that satisfy their taste. Next, the cost ratio between recommended and intended basket costs is calculated as an objective function:

$$J_2(\mathbf{x}, \mathbf{x}^*) = \rho_2(\mathbf{x}, \mathbf{x}^*). \quad (4)$$

The intended basket does not minimize Relation (4), whereas a basket with no products at all would be the optimal solution.

Next, the nutritional values of a recommended basket are considered for optimization. For each unit of product i and nutritional product feature j the median nutritional quantity per unit $c_{i,j}$ is calculated. Three nutritional features are considered $j \in \{3, 4, 5\}$. The health objective functions use the intended basket nutritional value as a baseline to evaluate the difference for each nutritional feature between recommended and intended baskets:

$$J_j(\mathbf{x}, \hat{\mathbf{x}}) = (1 - \rho_j(\mathbf{x}, \mathbf{x}^*))^2 = \left(\frac{v_j(\mathbf{x}^*) - v_j(\mathbf{x})}{v_j(\mathbf{x}^*)} \right)^2, j \in \{3, 4, 5\} \quad (5)$$

The intended basket is one solution that minimizes the Relation (5).

2.2 Environmental Impact Objectives

Collective environmental values are also considered based on the provided data from Ref. [32]. In total, a set of six environmental impact criteria are considered for each product, as shown in Table 2, namely *green house gas* (GHG) emissions, which contribute to climate change, *acidifying* pollution that decreases fertility and can cause desertification, *eutrophication* pollution, which destabilizes food chains in ecosystems, *water usage* that has several environmental effects, *stress-weighted water* usage that takes into account whether the water is taken from

arid/dry lands, and *land usage*, which is important to resource allocation for farming and deforestation. The median product features per unit are used as coefficients $c_{i,j}$ for calculating $v_j, j > 5$. Similar to the price objective, the ratio between intended and recommended basket of each environmental impact feature is considered as an objective function:

$$J_j(\mathbf{x}, \mathbf{x}^*) = \rho_j(\mathbf{x}, \mathbf{x}^*) \quad (6)$$

It is important to note that for the current dataset, there are no negative values for any coefficient $c_{i,j}$, thus all nominators and denominators of the proposed objectives are positive. Unless the intended basket optimizes all of the above objectives simultaneously and is non-empty, then there is no solution that optimizes the above objectives simultaneously. For example this can be shown when removing a single item from a non-empty intended basket. The item removal will decrease the price objective value and also environmental impact objectives, while it will increase the taste objective value.

2.3 Problem Formulation

The proposed optimization framework evaluates the recommended baskets across a set $C = \{1, 2, \dots, M\}$ of all $M=11$ different objectives presented above. The optimization is performed in a decentralized manner and only uses the intended basket to decide objective function values. The multi-objective problem for M objectives can be summarized as

$$\min_{\mathbf{x}} (J_1(\mathbf{x}, \mathbf{x}^*), J_2(\mathbf{x}, \mathbf{x}^*), \dots, J_M(\mathbf{x}, \mathbf{x}^*)), \quad \mathbf{x} \in \hat{X} \quad (7)$$

for a set of feasible baskets \hat{X} . An optimization algorithm $f(X_0; \mathbf{w}) = X$ with parameter vector \mathbf{w} takes an initial set of baskets X_0 and calculates a recommended set of baskets X . The goal of such algorithm is to find a non-dominated set of baskets. A basket \mathbf{x} dominates $\mathbf{x} \prec \mathbf{x}'$ another basket \mathbf{x}' if $J_j(\mathbf{x}) \leq J_j(\mathbf{x}')$ for all $j \in C$ and $J_j(\mathbf{x}) < J_j(\mathbf{x}')$ holds at least for one j [10]. If no other basket dominates \mathbf{x} , then it is referred as non-dominated.

3 Evolutionary Algorithms and Multi-Objective Optimization

Evolutionary strategies are widely used for multi-objective optimization [11] with $M \geq 2$ objectives. A brief overview is illustrated in Figure 1a. Typically each basket, or solution¹ in the optimization context, \mathbf{x} is mapped to an objective vector $\boldsymbol{\zeta}(\mathbf{x}) \in \mathbb{R}^M$, where each vector element represents an objective function value $\zeta_j = J_j(\mathbf{x})$. Often, such strategies improve a set of an initial population of solutions X_τ by applying probabilistic operators on each solution vector \mathbf{x} ,

¹The term solution will be used in the sections that describe models in accordance to literature.

such as the *random crossover*. Random crossover randomly combines elements from different solutions \mathbf{x}, \mathbf{x}' with probability p

$$x_i = \begin{cases} x'_i & \text{if } \delta < p \\ x_i & \text{otherwise} \end{cases}, \quad (8)$$

where δ is sampled from a probability density function $\delta \sim f$ with finite support $[0, 1]$. Another probabilistic mechanism is the *random mutation*, e.g. replacing an element of the solution with a random number sampled from a probability distribution $\kappa \sim f_{\text{discrete}}$ to an element of the solution

$$x_i = \kappa. \quad (9)$$

Each new solution is evaluated based on the corresponding objective vector $\zeta(\mathbf{x})$ and a *selection* of solutions is performed. Typically a non-dominated sorting is performed for the selection of non-dominated solution candidates both from new solutions and the initial population. The non-dominated sorting is performed recursively, i.e. each time a non-dominated set F_α is selected, the non-dominated solutions are assigned to F_α and then removed from the population. A new non-dominated search is performed on the remaining solutions to determine the non-dominated front $F_{\alpha+1}$. This process repeats until all solutions are assigned to a front. A possible selection mechanism would select all non-dominated solutions, i.e. the solutions in F_1 . The selected solution candidates are preserved in a new population of solutions $X_{\tau+1}$ and the whole process (crossover, mutation, selection) is repeated until a convergence criterion is met, e.g. no new solutions are preserved in a population after an iteration. Often τ is referred to as a *generation*. A widely used algorithm that follows the above strategy for multi-objective optimization is the Non-dominated Sorting Genetic Algorithm II (NSGA-II) [10].

3.1 Gradient Guided Genetic Algorithm

Probabilistic strategies are often criticized for slow convergence time [22], especially on high dimensional problems, and dependence on randomness [18, 27]. Recently, deterministic chaos genetic algorithms have been proposed to calculate solutions in a deterministic and seemingly in a more efficient manner [39, 41]. Furthermore, chaotic maps seem very promising for sparse and highly dimensional problems as they can control entropy [18] and the performance of the optimization procedures. For example, genetic algorithms may show improved performance if a logistic map [18] is used to sample initial solutions around the intended basket. Nevertheless, chaos genetic algorithms do not use explicit feedback from the loss function, such as Multi-Objective Natural Evolution Strategies [19] (MO-NES), and often the selection of adequate chaotic maps requires extensive hyper-parameter optimization [18, 27]. This article investigates another potential design, where neural networks are used to perform *mutation and crossover* operators and/or *initialize the population* instead

of chaotic maps. Neural networks show promising capabilities to learn chaotic maps and strange attractors [26], and back-propagation can be used to learn the parameters of the neural networks and control the chaotic behavior to improve solutions across generations.

Next, an overview of G3A is provided based on Figure 1b, but more technical details can be found in the Appendix Section D. An initial population matrix \mathbf{X}_0 is calculated by applying the untrained neural mutation from $t = 0$ to $t = T$. B solutions are selected during initialization, by sampling the mutation trajectory every $\Delta t = T/B$. During each generation, a population matrix $\mathbf{X}_\tau \in \mathbb{N}_0^{B \times N}$ is created, where each row represents a recommended solution.

A neural crossover operator is then applied on the population matrix and generates an offspring solution for each solution in the initial population. The main neural network component is a transformer network $f_{\text{transformer}} : \mathbb{N}_0^{B \times N} \rightarrow \mathbb{R}^{B \times B \times N}$ with Gaussian Error Linear Unit [21] (GeLU) activation functions as hidden layers [37]. Each parent solution \mathbf{x} is compared with the rest of the population matrix \mathbf{X}_τ . For each element x_i of the parent solution, the transformer generates an attention vector $\mathbf{g} \in \mathbb{R}^B$ over all solutions in the population. The element $\hat{x}_{i,b}$ is selected from the b -th parent in the population that received the maximum attention value from the transformer $b = \arg \max_b g_b$. A sigmoid activation is then applied on the attention values and each selected parent element is used to calculate an ‘‘offspring’’ solution element x'_i in the following manner:

$$x'_i = \text{sigmoid}(g_k)x_i + (1 - \text{sigmoid}(g_b))\hat{x}_{i,b}. \quad (10)$$

Next, a mutation operator neural network $u(\mathbf{x}(t)) : \mathbb{R}^{B \times N} \rightarrow \mathbb{R}^{B \times N}$ evolves a solution $\mathbf{x}(t)$ in continuous time t by applying the following neural ODE control

$$\dot{\mathbf{x}}(t) = \mathbf{u}(\mathbf{x}(t)). \quad (11)$$

A neural ODE solve [8] scheme is used to calculate the continuous time evolution between subsequent genetic generations, e.g. $\mathbf{x}(0) \rightarrow \mathbf{x}(T)$. The underlying neural network has sinusoidal activation functions in the hidden layer, inspired by the sinusoidal iterator used in Ref. [27]. To select the solutions that are preserved to the next generation, a finite number of mutated solution is sampled uniformly across time for each solution $\mathbf{x}(0)$ of the current generation τ at predetermined time-steps within the ODE solver. The output activation of the neural network is a Rectifier Linear Unit (ReLU) activation [37], which removes negative product quantities from each solutions.

Neural network weights and activation functions generate real-valued solutions. The proposed problems require discrete product quantities in the solution. Therefore, a discretization operation that allows gradient propagation is applied on each solution. A novel discretization scheme, termed fractional decoupling, is used and is described in detail in Section C. This scheme allows for gradient propagation during training, in comparison to rounding operators.

A non-dominated sorting is performed across all discretized solutions to determine the best solutions from each trajectory. The mean objective value per

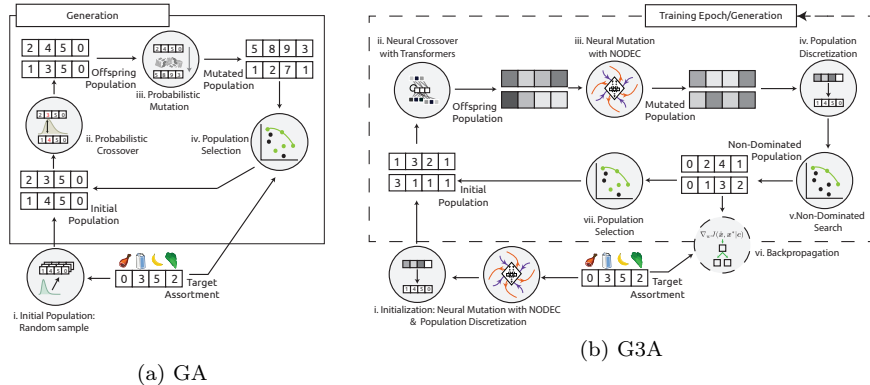


FIGURE 1: A high level illustration of the G3A and the classic GA. In the classic GA (a), the components of initial population sampling (a.i), crossover (a.ii), and mutation (a.iii) are often performed in a probabilistic manner. The population selection (a.iv) applies various mechanisms, such as a non-dominated sorting, over the current population to select the solutions that will continue in the next generation. Often a subset of the non-dominated solutions is preserved to the next generation. In G3A (b.) the initial population sample (b.i), the crossover (b.ii), and mutation operators (b.iii) are performed with a neural network. A discretization technique that allows back-propagation is then applied (component b.iv), and then a gradient descent update is performed based on the loss values of all non-dominated solution (components b.v-b.vi). Population selection (b.vii) happens after the network update, thus gradient guided genetics preserves information from all non-dominated solutions in its weight.

feature

$$\bar{\zeta}_j = \frac{\sum_{\mathbf{x}(t) \in F_1} \zeta_j(\mathbf{x}(t))}{|F_1|} \quad (12)$$

is calculated over all non-dominated solutions, i.e. all samples $\mathbf{x} \in F_1$, and then each element $\bar{\zeta}_j$ is used to calculate gradients and perform the parameter update. Mean objective values $\bar{\zeta}_j$ can be scaled before gradient calculation to match user preferences and guide the algorithm towards non-dominated solutions that are better performing in specific objective values. To select the B solutions that are used as input population for the next generation, the hyper-volume and non-dominated ranks are used [19] as described in the MO-NES baseline in Appendix section D.6.2. More technical details on training schemes, network architectures are found in the Appendix Section D.

4 Experimental Evaluation

Two multi-objective optimization strategies are compared with G3A, namely MO-NES and reference point NSGA-II [9] (RNSGA-II). Both baselines are described in more detail in Section D.6. All baselines are evaluated in weekly basket purchases that happen over the course of 85 weeks for 500 households,

and in total 28400 intended baskets are considered. In particular, the households are chosen based on their total green house gasses (GHG) emissions, i.e. the top 500 emission producers are selected. G3A is parameterized to generate $B = 8$ recommendations per intended basket, whereas RNSGA-II and MO-NES generate $B = 10$ recommendations per intended basket. The population sizes were chosen after evaluating different values. The sizes that generated well-performing solutions efficiently were preferred. For each recommendation, a ratio towards the cost, environmental impact, or nutritional quantities of the intended basket are considered. Some of the ratio functions coincide with the proposed objective functions, but this is not the case for nutritional losses, as the normalized MSE showed better convergence, but required scaling.

It is important to note that all three baselines were tested on a subset of potential hyper-parameters. Hyper-parameter optimization was performed for several days to the extent that each method was able to solve the problem effectively. From observed models, the best performing parameterization per method was selected. In future work, G3A will be compared against other optimization methods on more established problems to determine performance in terms of optimality. Such a study was out of the scope of this article.

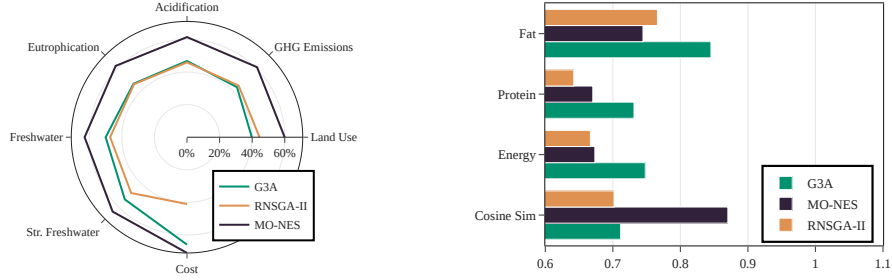
4.1 Recommendation Comparison

First, the ability of baselines to produce non-dominated solutions for the problem is evaluated. Table 4 contains a comparison where all recommendations for an intended basket \mathbf{x}^* from all methods are compared against each other and only the non-dominated solutions are kept across all methods. The ratio of total dominated solutions divided by total recommendations per method is calculated. All three baselines produce diverse non-dominated solutions, as they all achieve high mean ratio of non-dominated to total recommended baskets per intended basket. This indicates that the problem can be tackled effectively by all methods.

Model	Mean	Mean CI	Median	Median CI
G3A	0.980	(0.979, 0.981)	1.0	(1.0, 1.0)
MO-NES	0.948	(0.946, 0.949)	1.0	(1.0, 1.0)
RNSGA-II	0.986	(0.985, 0.986)	1.0	(1.0, 1.0)

TABLE 4: Mean and median values of non-dominated percentage of solutions when recommendations from all methods are combined together. Reverse bootstrap confidence intervals with significance level $\alpha = 0.05$ are also provided. All three baselines find a high percentage of non-dominated solutions, even when compared to each other.

Several recommended baskets per model may have non-preferred objective values. For example, a solution may achieve the optimal value in terms of a nutritional loss and then be selected as a non-dominated solution, although it



(a) Cost and Environmental Impact Ratios (lower values - points closer to center are preferred).

(b) Nutritional ratios and cosine similarity (higher values - longer bars are preferred).

FIGURE 2: A comparison of cosine similarity and the total emission, nutritional, and cost of a recommendation, as a ratio to the corresponding intended basket. For each baseline the mean ratio value over all recommendations that achieve cosine similarity higher than 0.5 and have all environmental ratios costs below 1.0 are considered.

produces 200% more emissions. Such solutions are discarded for the comparisons in the next sections, i.e. not recommended. A filtering is applied by discarding any solution that has a cost or any environmental impact quantity or cost ratio $\rho(\mathbf{x}, \mathbf{x}^*) \geq 1.0$. Furthermore, very dissimilar baskets are also discarded, i.e. when $\text{cosine_sim}(\mathbf{x}, \mathbf{x}^*) \leq 0.5$. For each recommendation the cosine similarity and environmental impact, nutritional and cost ratios towards the corresponding intended basket are calculated. The mean value of the ratio calculations over all recommendations per model are reported in Figure 2. Figure 2 indicates that RNSGA-II outperforms other baselines in terms of cost, while G3A shows higher performance in terms of nutritional values. MO-NES shows higher performance in terms of cosine similarity. As indicated by the dominance analysis results, all models can provide highly dominant solutions, that potentially specialize better in subsets of objectives. Depending on the design goals of the system or the priority of the individual, a different algorithm might be more preferred. Furthermore, all three models can be further altered to include consumer input in which objectives need to be prioritized. For G3A and MO-NES this can be implemented by adding weights and scaling the objective function values before the gradient update. For RNSGA-II this can be achieved by creating reference points that correspond to the user priorities.

Model	Elapsed Wall Clock Time seconds	GHG Emissions kg CO ₂ eq.	Mean, Min GHG Emission Improvement kg CO ₂ eq.
G3A (GPU)	1.89 ± 1.22	$2.07 \pm 1.44)e-08$	31.49, 0.46
MO-NES (CPU)	0.20 ± 0.01	$(2.16 \pm 0.14)e-09$	21.03, 0.41
RNSGA-II (CPU)	0.46 ± 0.06	$(6.95 \pm 2.41)e-10$	34.04, 0.45

TABLE 6: Execution time and GHG emissions (mean \pm standard deviation) measured with python and the codecarbon library [33] over a sample of 100 intended baskets from different households. The mean and minimum GHG emission improvement for accepting a single recommendation is also reported to outline the potential cost-benefit of accepting versus calculating recommendations.

4.2 Calculation Execution Time and Emissions

A sample of 100 intended baskets over a single week is used to determine execution time and calculation GHG emission for each model (see Table 6). Although G3A requires higher computation time and generates more emissions per calculation of recommendations, all models produce emissions and wall clock times are not significant. Accepting a single recommendation of any model can justify the emissions of thousands or even millions of calculations of other recommendations. Furthermore, G3A code is still at an experimental level, and better code optimization can be achieved to further reduce calculation times and emissions.

4.3 Real-World Impact

To extend the comparison of G3A and estimate the impact on total reduction values, a counterfactual scenario is evaluated. For each model, 5000 counterfactual trajectories are sampled, each trajectory being 86 weeks long. For each trajectory, it is assumed that 25% of all intended baskets are replaced with a recommendation. The recommendation which replaces the intended basket is chosen randomly². Figure 3 illustrates the ability of all algorithms to achieve a considerable reduction of environmental impact compared to the intended basket. For example, deciding to replace 25% of intended baskets with a G3A recommendation leads to a reduction of approximately 35 metric kilo-tons of CO₂ eq. or approximately 1 billion litres of stressed freshwater for G3A. The

²In the current setting, a decision model for sampling, such as the one in [25] cannot be used, because the transactions of the current dataset may be effected by marketing campaigns and other covariates. Furthermore, it is not apparent of whether consumers were aware of sustainability issues when performing a purchase, thus the modeling of environmental impact decision factors may be invalid. Thus, designing a valid decision model to estimate the effect of a recommender system in this case is out of scope of this article and could potentially be considered as future work.

current results indicate that G3A achieves similar performance to RNSGA-II, but by removing less and adding more products. MO-NES instead produces recommendations that have the least impact on the consumer basket.

5 Conclusion

This article showcases a multi-objective approach to sustainable recommendations, where value-sensitive design is also taken into account. The problem of finding sustainable personalized baskets is evaluated with objectives and constraints derived from real-world data. Existing baselines are compared with a novel gradient guided genetic algorithm (G3A) and results showcase that all considered models produce good solutions to the problem. Even when individuals would adopt a fraction of the sustainable recommendations, a considerable environmental impact can be observed.

From a technical perspective this paper introduces a novel multi-objective optimization algorithm that has comparable performance with state-of-the-art baselines on the new task. To make this happen, existing techniques from evolutionary methods are combined with state-of-the-art neural network architectures and a novel discretization technique, termed fractional decoupling. This technique allows for efficient gradient propagation when neural networks are applied to mixed integer programming problems, such as the one presented in this paper.

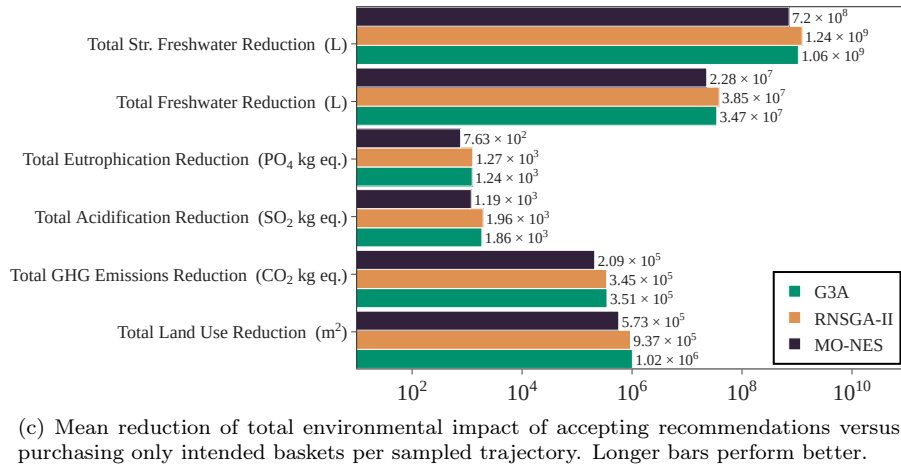
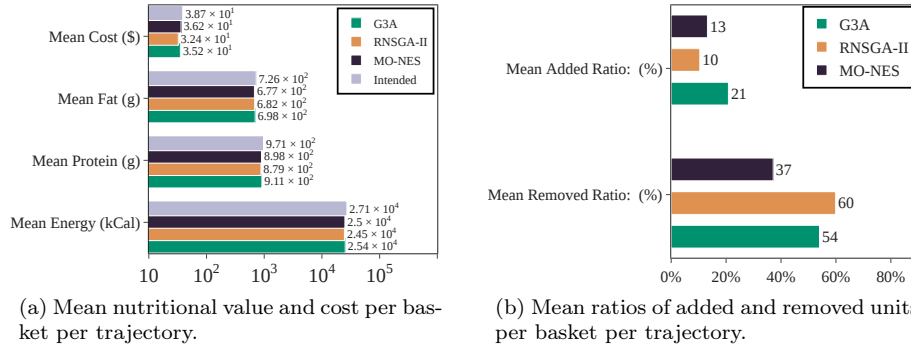


FIGURE 3: Comparison of the impact per model over 5000 trajectories, where 25% of the intended basket purchases is randomly replaced with a recommendation. Mean nutritional quantities per basket and trajectory are reported (see a.). Next (see b.), the mean value of added and removed units per basket are provided over all recommendations and trajectories, where intended baskets are omitted for the calculation. The total environmental impact and cost reduction are calculated per sample and then subtracted from the total quantities of the original trajectory (only intended baskets are purchased). Although confidence intervals are calculated, they are omitted as they are mostly too narrow and, thus, not visible.

References

- [1] Ricardo Abejón et al. “Multi-Objective Optimization of Nutritional, Environmental and Economic Aspects of Diets Applied to the Spanish Context”. In: *Foods* 9.11 (2020), p. 1677.
- [2] Thomas Asikis, Lucas Böttcher, and Nino Antulov-Fantulin. *Neural Ordinary Differential Equation Control of Dynamics on Graphs*. 2021. arXiv: 2006.09773 [cs.LG].
- [3] Thomas Asikis et al. “How value-sensitive design can empower sustainable consumption”. In: *Royal Society open science* 8.1 (2021), p. 201418.
- [4] J. Blank and K. Deb. “pymoo: Multi-Objective Optimization in Python”. In: *IEEE Access* 8 (2020), pp. 89497–89509.
- [5] Lucas Böttcher, Nino Antulov-Fantulin, and Thomas Asikis. “Implicit energy regularization of neural ordinary-differential-equation control”. In: *arXiv preprint arXiv:2103.06525* (2021).
- [6] WJ Wouter Botzen and Jeroen CJM van den Bergh. “How sensitive is Nordhaus to Weitzman? Climate policy in DICE with an alternative damage function”. In: *Economics Letters* 117.1 (2012), pp. 372–374.
- [7] Abhishek Chaudhary, David Gustafson, and Alexander Mathys. “Multi-indicator sustainability assessment of global food systems”. In: *Nature communications* 9.1 (2018), p. 848.
- [8] Ricky T. Q. Chen et al. “Neural Ordinary Differential Equations”. In: *Advances in Neural Information Processing Systems* (2018).
- [9] Kalyanmoy Deb and J Sundar. “Reference point based multi-objective optimization using evolutionary algorithms”. In: *Proceedings of the 8th annual conference on Genetic and evolutionary computation*. 2006, pp. 635–642.
- [10] Kalyanmoy Deb et al. “A fast and elitist multiobjective genetic algorithm: NSGA-II”. In: *IEEE transactions on evolutionary computation* 6.2 (2002), pp. 182–197.
- [11] Kalyanmoy Deb et al. “A fast elitist non-dominated sorting genetic algorithm for multi-objective optimization: NSGA-II”. In: *International conference on parallel problem solving from nature*. Springer. 2000, pp. 849–858.
- [12] Jacob Devlin et al. “Bert: Pre-training of deep bidirectional transformers for language understanding”. In: *arXiv preprint arXiv:1810.04805* (2018).
- [13] Virginia Dignum. *Responsible artificial intelligence: how to develop and use AI in a responsible way*. Springer Nature, 2019.
- [14] *Dunnhumby - The complete journey dataset*. Available at <https://www.dunnhumby.com/source-files/> (last accessed: September 2021). 2021.

- [15] *FAO – Food Agriculture Organization, Food Balance Sheets*. Available at <http://www.fao.org/3/X9892E/X9892e05.htm> (last accessed: September 2021). 20211.
- [16] Frank Figge, William Young, and Ralf Barkemeyer. “Sufficiency or efficiency to achieve lower resource consumption and emissions? The role of the rebound effect”. In: *Journal of Cleaner Production* 69 (2014), pp. 216–224.
- [17] Carlos M Fonseca, Luís Paquete, and Manuel López-Ibáñez. “An improved dimension-sweep algorithm for the hypervolume indicator”. In: *2006 IEEE international conference on evolutionary computation*. IEEE. 2006, pp. 1157–1163.
- [18] Guillermo Fuertes et al. “Chaotic genetic algorithm and the effects of entropy in performance optimization”. In: *Chaos: An Interdisciplinary Journal of Nonlinear Science* 29.1 (2019), p. 013132.
- [19] Tobias Glasmachers, Tom Schaul, and Jürgen Schmidhuber. “A natural evolution strategy for multi-objective optimization”. In: *International Conference on Parallel Problem Solving from Nature*. Springer. 2010, pp. 627–636.
- [20] Dirk Helbing and Evangelos Pournaras. “Build digital democracy A WISE KING?” In: *Nature* 527.7576 (2015), pp. 33–34. ISSN: 0028-0836. DOI: 10.1038/527033a.
- [21] Dan Hendrycks and Kevin Gimpel. “Gaussian error linear units (gelus)”. In: *arXiv preprint arXiv:1606.08415* (2016).
- [22] Hisao Ishibuchi et al. “Evolutionary many-objective optimization by NSGA-II and MOEA/D with large populations”. In: *2009 IEEE International Conference on Systems, Man and Cybernetics*. IEEE. 2009, pp. 1758–1763.
- [23] Eric Jang, Shixiang Gu, and Ben Poole. “Categorical reparameterization with gumbel-softmax”. In: *arXiv preprint arXiv:1611.01144* (2016).
- [24] A Kelly, W Becker, and E Helsing. “Food balance sheets”. In: *Food and health data: their use in nutrition policy-making*. Copenhagen: WHO Regional Office for Europe (1991), pp. 39–47.
- [25] Kyuseop Kwak, Sri Devi Duvvuri, and Gary J Russell. “An analysis of assortment choice in grocery retailing”. In: *Journal of Retailing* 91.1 (2015), pp. 19–33.
- [26] Ziwei Li and Sai Ravela. “Neural Networks as Geometric Chaotic Maps”. In: *IEEE Transactions on Neural Networks and Learning Systems* (2021).
- [27] Hui Lu et al. “The effects of using chaotic map on improving the performance of multiobjective evolutionary algorithms”. In: *Mathematical Problems in Engineering* 2014 (2014).
- [28] Talha Manzoor et al. “Optimal control for sustainable consumption of natural resources”. In: *IFAC Proceedings Volumes* 47.3 (2014), pp. 10725–10730.

- [29] R.T. Marler and J.S. Arora. “Survey of multi-objective optimization methods for engineering”. In: *Structural and Multidisciplinary Optimization* 26.6 (2004), pp. 369–395. ISSN: 1615-1488. DOI: 10.1007/s00158-003-0368-6.
- [30] TPL Nghiem and LR Carrasco. “Mobile applications to link sustainable consumption with impacts on the environment and biodiversity”. In: *BioScience* 66.5 (2016), pp. 384–392.
- [31] William D Nordhaus. “Optimal greenhouse-gas reductions and tax policy in the " DICE" model”. In: *The American Economic Review* 83.2 (1993), pp. 313–317.
- [32] Joseph Poore and Thomas Nemecek. “Reducing food’s environmental impacts through producers and consumers”. In: *Science* 360.6392 (2018), pp. 987–992.
- [33] Victor Schmidt et al. *CodeCarbon: Estimate and Track Carbon Emissions from Machine Learning Computing*. <https://github.com/mlco2/codecarbon>. 2021. DOI: 10.5281/zenodo.4658424.
- [34] Sabina Tomkins et al. “Sustainability at scale: towards bridging the intention-behavior gap with sustainable recommendations”. In: *Proceedings of the 12th ACM Conference on Recommender Systems*. ACM, 2018, pp. 214–218.
- [35] Christian P Traeger. “A 4-stated DICE: quantitatively addressing uncertainty effects in climate change”. In: *Environmental and Resource Economics* 59.1 (2014), pp. 1–37.
- [36] UN. *Global Sustainable Development Report: 2015 edition*. Tech. rep. United Nations, 2015, p. 202.
- [37] Ashish Vaswani et al. “Attention is all you need”. In: *Advances in Neural Information Processing Systems*. Curran Associates, Inc., 2017, pp. 5998–6008.
- [38] Ricardo Vinuesa et al. “The role of artificial intelligence in achieving the Sustainable Development Goals”. In: *Nature communications* 11.1 (2020), pp. 1–10.
- [39] Xuefeng F Yan, Dezhao Z Chen, and Shangxu X Hu. “Chaos-genetic algorithms for optimizing the operating conditions based on RBF-PLS model”. In: *Computers & Chemical Engineering* 27.10 (2003), pp. 1393–1404.
- [40] Penghang Yin et al. “Understanding straight-through estimator in training activation quantized neural nets”. In: *arXiv preprint arXiv:1903.05662* (2019).
- [41] You Yong, Sheng Wanxing, and Wang Sunan. “Study of chaos genetic algorithms and its application in neural networks”. In: *2002 IEEE Region 10 Conference on Computers, Communications, Control and Power Engineering. TENC0M’02. Proceedings*. Vol. 1. IEEE, 2002, pp. 232–235.

- [42] Eckart Zitzler and Lothar Thiele. “Multiobjective optimization using evolutionary algorithms—a comparative case study”. In: *International conference on parallel problem solving from nature*. Springer. 1998, pp. 292–301.
- [43] Yi Zuo et al. “Personalized recommendation based on evolutionary multi-objective optimization [research frontier]”. In: *IEEE Computational Intelligence Magazine* 10.1 (2015), pp. 52–62.

Appendix A Data Availability

Dunnhumby transactions and data are downloaded from Ref [14]. Food Agricultural Organization Food Balance sheets are taken from Ref. [15]. The environmental impact data are taken from Ref. [32]. Finally, all the data generated in this study are openly accessible, so please follow the instructions in www.github.com/asikist/g3a/data.

Appendix B Code Availability

Code is available in Github www.github.com/asikist/g3a

Appendix C Fractional Decoupling

The personalized sustainable basket problem is presented as a mixed integer programming problem (MIP). Therefore, discrete outputs for the proposed optimization schemes are considered. Neural networks are known to operate in real value settings, as back-propagation requires the output of neural networks to be continuous and differentiable in regards to objective, so that the chain rule can be efficiently applied. Unfortunately, this is not the case for MIP schemes.

In a typical neural network feed-forward setting, output of the neural network is denoted with as a weight vector \mathbf{w} as \mathbf{y} and its input as a \mathbf{x} . The main challenge is to achieve gradient back-propagation when facing the integer output problem. More specifically when one could apply a floor rounding on output elements y_i by subtracting the fractional part $h_i = y_i - \lfloor y_i \rfloor$, i.e. the difference between y and the closest lower integer value $\lfloor y_i \rfloor$. When rounding to the lower closest integer, the neural network output is transformed as follows:

$$f(\mathbf{x}; \mathbf{w}) = \mathbf{y} - \mathbf{h} \tag{13}$$

where, \mathbf{h} is the vector of the fractional parts of \mathbf{y} . The main challenge for back-propagating error from the above operation is the calculation of the gradient of Relation (13) is that the floor function is not differentiable in its domain, in particular at the integer values (see Figure 4).

A potential approach is to train the neural networks in a real valued manner and then apply rounding when evaluating the solutions. In the specific case, this proves problematic, as many product quantities end up being rounded to 0, yielding empty baskets as solutions. Another approach proposed in literature is to use the Gumbel soft-max operator [23], which allows for gradient propagation via the so-called straight through estimators [40]. Since the decision problem in question requires no upper bounds on purchased product quantities, using the Gumbel soft-max operator may yield highly dimensional outputs that may take considerable more time to train for large scale problems.

An alternative approach, termed fractional decoupling, is proposed to efficiently calculate a gradient update and perform gradient descent. To perform

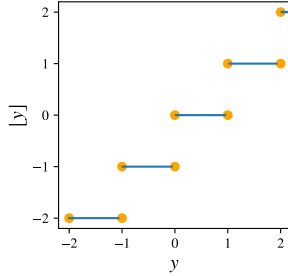


FIGURE 4: A plot of the floor function for $x \in [-2, 2]$. Orange points indicate the regimes, where the floor function is not differentiable.

fractional decoupling, one simply subtracts the fractional part h_i of a real valued output y_i , while treating it as constant, i.e. this allows no gradient propagation through the fractional part in the computational graph, similar to bias terms or physics inspired neural networks constants.

Proposition 1. *Decoupling the fractional part h of real value $y \in \mathbb{R}$ from the gradient calculations allows for feed-forward rounding and well-defined gradient propagation when the loss function is differentiable w.r.t. to y in $[\min(y - h), \max y_i]$*

Proof. The fractional part h is considered constant, that is no gradient propagation is allowed through it when calculating gradients. For a network parameter w_k , the gradient calculated after applying the above operation will have the following form

$$\frac{\partial J(y - h)}{\partial w_k} = \frac{\partial J(y - h)}{\partial (y - h)} \frac{\partial y - \partial h}{\partial w_k}. \quad (14)$$

Since h is treated as a constant $\partial h = 0$

$$\frac{\partial J(y - h)}{\partial w_k} = \frac{\partial J(y - h)}{\partial (y)} \frac{\partial y}{\partial w_k} = \frac{\partial J(y - h)}{\partial w_k}. \quad (15)$$

The resulting gradient corresponds to the original gradient of the loss function shifted to the nearest integer neural network output $y - h$, which is well defined given the theorem assumption. \square

The above proof can be respectively extended to any rounding operator, such as ceiling or half-up. The introduced fractional decoupling technique effectively allows gradient flows through discretization operators in order to facilitate learning.

C.1 Numerical Example of Discretized Gradient Flows

To illustrate the gradient discretization of fractional decoupling, an illustrative example is provided, which compares gradient flows of a 2-parameter network

both with and without fractional decoupling when solving the same problem. Given a predetermined coefficient vector $\hat{\mathbf{w}} = [\hat{w}_1 \ \hat{w}_2] = [4 \ 1]$ and normally distributed inputs $x_1, x_2 \sim \mathcal{N}(\mu = 0, \sigma = 1)$, apply the following transformation is applied:

$$\hat{\mathbf{y}} = \lfloor \hat{\mathbf{w}} \odot \mathbf{x} \rfloor \quad (16)$$

Given a batch matrix of $M = 50$ input row vectors $X \in \mathbb{R}^{M \times N}$ with $N = 2$ features columns and their corresponding label matrix $\hat{Y} \in \mathbb{R}^{M \times 1}$, two neural networks are trained. A neural network with continuous outputs during training, where the floor function is applied only during inference:

$$\mathbf{f}_1(\mathbf{x}) = \mathbf{y} = \mathbf{w} \odot \mathbf{x} \quad (17)$$

and a separate neural network with a fractional decoupling term:

$$\mathbf{f}_2(\mathbf{x}) = \mathbf{y} - \mathbf{h}. \quad (18)$$

The mean squared loss is minimized during learning over a single batch of $M = 50$ samples:

$$J(\mathbf{f}(\mathbf{x})) = \frac{1}{M} \sum_1^M \frac{1}{2} \|\mathbf{f}_i(\mathbf{x}) - \hat{\mathbf{y}}\|_2^2. \quad (19)$$

For the experiments, 40 weight values evenly spaced in the interval $[0, 6]$ are considered for each neural network parameter $w_1 w_2$ and generate all possible pairs (cartesian product). For each parameter vector of $\mathbf{w} = (w_1 w_2)$ the gradients $\nabla_{\mathbf{w}} J(f_1)$ and $\nabla_{\mathbf{w}} J(f_2)$ are calculated respectively. The calculated gradients are illustrated in Figure 5, where it is observed that fractional decoupling approximates the underlying coefficient vector better. In general it is observed that using fractional decoupling has little effect on the gradient direction and magnitude. The minimum magnitude gradient points for each neural network are expected to be a local minima for J (see black disks in Figure 5). During inference, it is observed that fractional decoupling yields a lower loss value $J(\mathbf{y} - \mathbf{h}) \approx 0.02$ compared to the continuous neural network with floored output $J(\mathbf{y}) \approx 0.28$.

Appendix D Gradient Guided Genetics

Technical details for gradient guided genetics are found in this section. Each element of the gradient guided genetics depicted as a module Figure 1 is explained in more detail in the following sections.

D.1 Neural Crossover

For neural crossover, the use of transformers that use the attention mechanism [37] is considered. A typical transformer architecture receives two sequences $x_1 \in \mathbb{R}^N, x_2 \in \mathbb{R}^M$ as an input and outputs a real valued (logit) matrix $A = \mathbb{R}^{N \times M}$ that can be transformed to a probability matrix by applying a

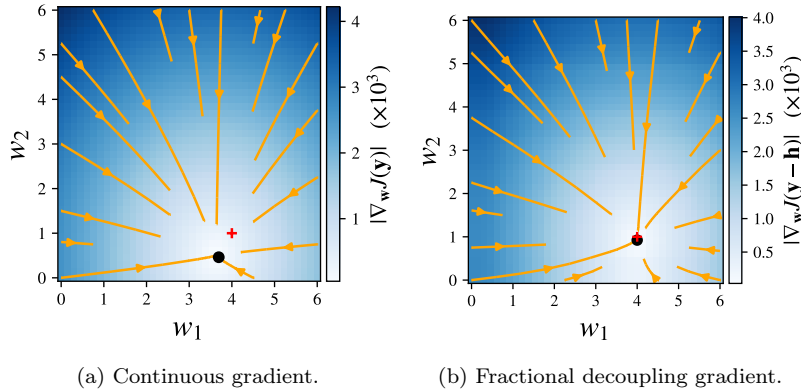


FIGURE 5: Gradient direction (orange lines), optimal solution (red cross) and lowest gradient norm point (black disk).

soft-max operator over its rows. The probability vector denotes the “attention” or assigned probability that an element from the second input sequence x_2 is important to match against the corresponding element i from sequence x_1 . Transformers are the state-of-the-art models used in several architectures that perform sequence matching related learning tasks, such as machine translation and text generation [12]. Often, multi-head attention mechanisms are used, where each “head” represents different neural network layers that focus “attention” on different parts of each sequence. In the current application, transformers are assumed to be able to naturally learn how to match parent chromosomes to optimize the goals. The output probability matrix is used to make a weighted average calculation between matched chromosomes as shown in Relation (10).

The multi-head attention transformer networks used in this work contain 1 encoder and 1 decoder layer with GeLU activation functions and 11 heads. Replacing the crossover network with probabilistic operators or simpler neural network architectures has not yielded better results so far, but is still a subject of study and future work. Both of the transformer encoder and decoder layers contain a hidden layer with 2048 hidden neurons and, layer norm layers in output and input and also dropout operations on neuron outputs, according to the default implementation found in <https://pytorch.org/docs/stable/generated/torch.nn.Transformer.html> (accessed October 2021). A sigmoid activation is used on the attention output to convert it in the range between $[0, 1]$.

D.2 Neural Mutation

The neural mutation operator follows the method proposed in Relation (11). The evolution period is $[0, 1]$ and a single hidden layer with 256 neurons. In total 9 mutated solutions are selected per trajectory. In the current setting, this parameterization yields high performing results, but in problem different

settings, higher mutation period value and other activation functions might work better. Replacing the mutation network with probabilistic operators or simpler neural network architectures has not yielded better results so far, but is still a subject of study and future work.

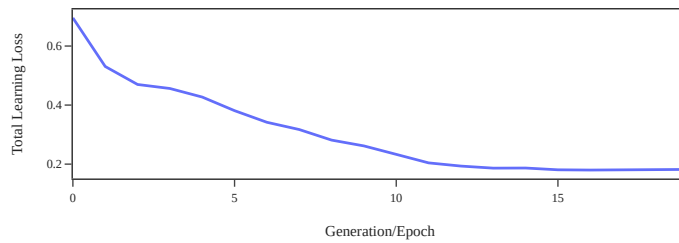
D.3 Population Discretization

Discretization of quantities in chromosomes is performed via fractional decoupling described in Section C. A ReLU function is applied to the real-valued chromosomes to preserve non-negative quantities. Then a fractional decoupling rounding is performed on the outcome. The back-propagation of fractional decoupling is confirmed by observing the parameter changes and loss convergence over time in Figure 6.

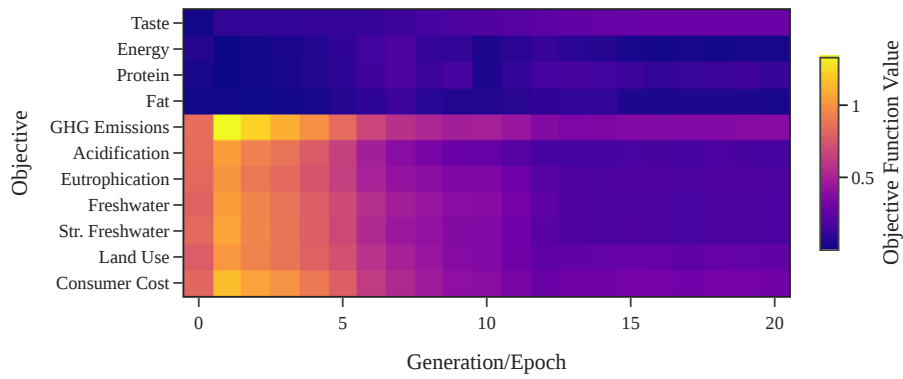
D.4 Back-Propagation Through Evolution

The back-propagation through evolution starts by calculating the individual objective function values for each solution selected by the selection operator. For each objective, the mean value over all selected individuals is calculated. Experimental results indicate that using a different optimizer for each Neural Operator yields higher performance. The RMSProp optimizer is used with learning rate $\eta = 0.0001$ for the neural mutation operator and an RMSProp optimizer with learning rate $\eta = 0.0001$ for the Neural Crossover Operator. The gradient is calculated per objective, and for health objectives the loss is scaled 7 times. Not scaling the loss yielded recommendations that did not optimize health objectives well.

A “stopping criterion” is calculated in the following manner in each generation. as the mean over all non-dominated solution objectives. The “stopping criterion” value is preserved for last three generations, and the mean value of the current generation is compared against the mean value of the last three generations “stopping criteria”. If the current “stopping criterion” differs less than 0.001 from the mean of the previous “stopping criteria”, the optimization is terminated. Learning convergence of the total loss and individual losses are found in Figure 6.



(a)



(b)

FIGURE 6: Learning loss (line) and normalized median values of the separate objective functions (heatmap) over the non-dominated chromosomes of each generation, for a single basket recommendation. As generations evolve, G3A converges all losses and the learning objective to lower (darker blue) values. If no convergence criterion is used, G3A may over-fit and produce solutions that optimize all objectives except Taste. This behavior was also observed in other baselines, and thus the cosine similarity filter was used.

D.5 Nomenclature

TABLE 7: Nomenclature part I

N	Number of distinct products and chromosome/solution length for the genetic.
\mathbf{x}	A non-negative integer vector $\mathbf{x} \in \mathbb{Z}_0^N$ representing a basket of product quantities.
\mathbf{x}^*	A purchased/intended basket used as the target basket for optimizing consumer taste.
j	A decision criterion/feature quantity.
$c_{i,j}$	A product feature quantity (e.g. kg of emissions) per unit of product i and feature j .
$v_j(\mathbf{x})$	The total quantity for a feature j quantity per basket.
\mathbf{x}'	A non-negative integer vector $\mathbf{x}' \in \mathbb{Z}_0^N$ representing another basket of product quantities.
$\rho_j(\mathbf{x}, \mathbf{x}')$	The ratio of total feature quantities $v_j(\mathbf{x}), v_j(\mathbf{x}')$ between two baskets \mathbf{x}, \mathbf{x}' .
$\ \cdot\ $	The L2 norm of a vector.
x_i	Quantity of product i in basket \mathbf{x} .
$J_j(\mathbf{x})$	The objective loss calculated for a basket \mathbf{x} and objective j . More than one inputs may be provided.
C	The set of criteria j with cardinality $ C = M$.
X	The set of solutions/baskets \mathbf{x} . Also termed as population.
\hat{X}	The feasible set of solutions/baskets \mathbf{x} , i.e. solutions that exist.
\tilde{X}_0	The initial set of solutions/baskets \mathbf{x} , i.e. solutions that are further optimized to generate recommendations. The generation can also be used as index to the population.
$\mathbf{x} \prec \mathbf{x}'$	An operator denoting that solution/basket \mathbf{x} dominates \mathbf{x}' . The dominance operator can also be used to describe dominance for points of the objective space $\zeta(\mathbf{x}) \prec \zeta(\mathbf{x}')$, which typically represent solutions.
$\zeta(\mathbf{x})$	A vector containing all objective values for solution \mathbf{x} and indexed by j .
B	The population or solution set size.

TABLE 9: Nomenclature part II

\mathbf{w}	A parameter vector that is optimized to generate solutions.
f	An optimization algorithm that generates a set of solutions X given an input set of solutions tsx_0 and parameters \mathbf{w} .
δ	A probability sample to decide whether random crossover should happen.
p	A probability threshold to decide whether random crossover should happen.
f	Probability density function for sampling continuous values in $[0, 1]$.
κ	Value of discrete random mutation.
f_{discrete}	probability distribution function for sampling discrete values in κ .
F_α	The non-dominated frontier of rank <i>alpha</i> . F_1 contains all the non-dominated solutions of a population.
X	A population represented as a matrix.
\mathbf{g}	An attention vector for an element x_i , representing the attention values assigned to all elements x'_i in the population.
b	The index of the second parent that received the highest attention.
$\mathbf{u}(\mathbf{x}(t))$	The NODEC output that controls neural mutation.
T	The total time that continuous mutation is applied on a chromosome.
τ	The generation index, that corresponds a specific generation in genetic optimization process.
h_i	The fractional part of a real value $y_i \in \mathbb{R}$
$\lfloor y_i \rfloor$	The floor operation on a real value $y_i \in \mathbb{R}$.
J	The learning loss of a neural network.
w_k	A neural network parameter.

TABLE 11: Nomenclature part III

q	The week index.
k	The household index.
σ	denotes the variance of a normal distribution, and in the MO-NES case the corresponding parameter.
A	The matrix that represents a “covariance” related parameter in MO-NES.
Z	A sample vector, where each element is sampled from a zero-mean unit variance normal distribution. This vector is used in MO-NES.
η	is used for learning rate parameter. In MO-NES, three learning rate parameters are used for each parameter, namely: η_σ^+ , η_σ^- , η_A .

D.6 Other Baseline Algorithms

D.6.1 RNSGA-II

A non-dominated sorting algorithm may produce a large number of non-dominated solutions that are not preferable, e.g. solutions that optimize a single objective very well and not the others. To keep the population size B per generation constant, a secondary selection operation needs to be performed. Random selection is often undesired in problems that have multiple objectives [9], and thus a more sophisticated technique is preferred. Some probabilistic evolutionary strategies use a sorting operation to perform a secondary selection operation that guide the evolutionary processes towards preferred non-dominated solutions, e.g. non-dominated that optimize specific combinations of the objectives very well. A typical example that will be used as a baseline in the current study is reference point NSGA-II, abbreviated as RNSGA-II [9], which uses reference directions to guide evolution towards preferred solutions. In brief, one or more reference points are selected to guide the evolution. A reference point $\hat{\zeta}$ is generated by providing a vector of preferred objective values to the system. Each candidate solution receives two ranks determined by the non-dominated sorting and a distance metric from each reference point, i.e. lower distance values receive lower. Lower ranks are used to select the candidates for the next generation. This algorithm shows higher performance gains compared to NSGA-II to perform better on multi-objective problems with more than 2 objectives [9]. RNSGA-II is used as a baseline in the current study following the default implementation of [4].

A logistic map [18] is applied on the initial basket to generate the initial solution for RNSGA-II, improving performance considerably compared to other random initialization. Several reference points settings are tested for RNSGA-II. The current reference points provided to RNSGA-II are three, one that is calculated by using the infeasible optimum, where every loss is 0, one that minimizes all individual losses (e.g. all values for $j \leq 5$ are 0 and the rest are 1), and one that minimizes all environmental losses (e.g. all values for $j > 5$ are set to 0). Using less than 2 reference points resulted often in bad performance. Other reference point settings were tested on 100 intended baskets, such as using the one the intended basket or minimization of specific losses on smaller samples, but it was unclear whether better performance could be achieved by using them. The current reference point setup was chosen, as it provided the best performing dominance ratio when comparing to other baselines. Integer exponential crossover and polynomial mutation are used for the genetic operators. Finally, other settings were tested with $B = 100$, but were omitted due to lower dominance ratio, slower convergence times, large number of solutions, and difficulty to determine subsets of good solutions.

D.6.2 MO-NES

Another way to handle multi-objective optimization problems is the use of Multi-Objective Natural Evolution Strategies (MO-NES) [19], which use a gra-

dient guided search algorithm to find non-dominated solutions by parametrizing a probabilistic model (relies on sampling). The algorithm optimizes the parameters of a model that samples solutions from underlying distributions. For each solution, a sample vector $\mathbf{z} \in \mathbb{R}^N$ is generated, where each element is sampled from a normal distribution $z_i \sim \mathcal{N}(0, 1)$. A new solution \mathbf{x}' is calculated based on a parent solution $\mathbf{x}' = \mathbf{x} + \sigma \mathbf{A} \mathbf{z}$, where $\sigma \in \mathbb{R}$, $\mathbf{A} \in \mathbb{R}^{N \times N}$ are the co-variance related terms. Samples from the previous population X_τ and the new candidates \mathbf{x}' are combined into an intermediate population X' . Each solution $\mathbf{x} \in X'$ is assigned a rank α based on the non-dominated sorting. A secondary rank β is assigned to each solution based on the value of a hyper-volume metric [19, 42] in a descending order. To calculate the hyper-volume metric, a dominated reference point $\boldsymbol{\zeta}^{(0)} \in \mathbb{R}^M$ is selected in the objective space, such that all considered solutions $\mathbf{x} \in X'$ dominate this point $\boldsymbol{\zeta}(\mathbf{x}) \prec \boldsymbol{\zeta}^{(0)}$. The hyper-volume metric [42] is used to calculate the hyper-volume between each solution and the dominated reference point, e.g. by using the proposed implementation of Ref. [17]. The hyper-volume metric is calculated on normalized loss values, which are calculated by subtracting the mean and then dividing with the standard deviation over all solutions. The covariance related parameters \mathbf{A}, σ are updated with a gradient update. A modified version of MO-NES, where solutions are rounded and negative values are clipped to 0 prior to evaluation is used as a baseline in the current article. The initial value of each solution is sampled as $x_i = \text{ReLU}(x), x \sim \mathcal{N}(0, 0.2)$. Parameter $\sigma = 1/3$ and elements of A were initialized uniformly in $[0, 0.001]$. Following notation from Ref. [19], the learning rates for each parameter are $\eta_\sigma^+ = 0.01$, $\eta_\sigma^- = 0.01/5$ and $\eta_A = 0.01/4$. MO-NES trains up to 40 generations.

Appendix E Dataset

Transaction data, product prices, and purchased quantities were retrieved by "The Complete Journey Dataset" by the Dunnhumby grocery store [14]. The quantities are included in US imperial units and a conversion to metric system was done in the following manner: (i) Unit labels are identified and grouped together with regular expressions, e.g. "LB,lb, LBs" all represent the same label which denotes pounds. (ii) Weight and volumetric labels are separated and proper conversion coefficients are used to convert each unit to the corresponding metric unit used in the other datasets. (iii) Prices may change through time, so the median price per unit is calculated through time and over all stores to generate the price features used by all algorithms.

Environmental impact indicators for product types are taken from Ref. [32]. Nutrition information from Food Agricultural Organization Food Balance Sheets [24] are downloaded from Ref [15]. All three datasets contain different product type labels for each product. From "The Complete Journey Dataset" the "SUB_COMMODITY_DESC" column is treated as the product identifier. Each value of the column "SUB_COMMODITY_DESC" is matched against the "product category" column from FAO FBS dataset and the dataset column "product

category" from Ref [15]. The resulting dataset contains transaction prices, purchased quantities, environmental impact values, and nutritional info per transaction. Any other dataset with similar structure and more diverse product characteristics is compatible with the proposed method for finding more sustainable personalized baskets.